

# Defect modes caused by twinning in one-dimensional photonic crystals

Hynek Němec

*Laboratoire d'Hyperfréquences et de Caractérisation, Université de Savoie, 73376 Le Bourget du Lac Cedex, France, and Institute of Physics, Academy of Sciences of the Czech Republic, and Center for Molecular Systems and Biomolecules, Na Slovance 2, 182 21 Prague 8, Czech Republic*

Lionel Duvillaret and François Quemeneur

*Laboratoire d'Hyperfréquences et de Caractérisation, Université de Savoie, 73376 Le Bourget du Lac Cedex, France*

Petr Kužel

*Institute of Physics, Academy of Sciences of the Czech Republic, and Center for Molecular Systems and Biomolecules, Na Slovance 2, 182 21 Prague 8, Czech Republic*

Received February 28, 2003

Propagation of electromagnetic waves in a one-dimensional photonic crystal with a twin-defect—a periodicity break where one half of the photonic structure is a mirror image of the other one—is studied using a transfer-matrix method. This work is done in the general framework of photonic structures composed of isotropic materials exhibiting both dielectric and magnetic properties. Both polarizations of electromagnetic waves impinging at oblique incidence on the structure are considered. We derive analytical expressions for the frequency of defect modes and for the enhancement of the electromagnetic field inside the defect. In particular, we discuss possibilities of tuning of defect levels for a photonic crystal structure with a two-layer elementary cell. © 2004 Optical Society of America

*OCIS codes:* 230.1480, 050.2230.

## 1. INTRODUCTION

Since the pioneering work of Yablonovitch,<sup>1</sup> research in photonic crystals (PCs) has known an impressive expansion and covers a wide range of the electromagnetic spectrum from microwaves<sup>2</sup> to the visible.<sup>3</sup> Although many applications and developments have already appeared, some great challenges remain. Among them, the control of defect modes is of major interest for filtering applications, signal demultiplexing, etc. Several papers that treat either the microwave domain<sup>4,5</sup> or the optical domain<sup>6</sup> have already been published on that subject. However, the design of controllable defect modes in PCs requires predictive formulas for the frequency dependence of the defect modes on physical parameters of PCs. Conducting even numerical studies still remains difficult for two- and three-dimensional PCs,<sup>7,8</sup> and one-dimensional PCs are thus natural choices for analytical investigations because of their simplicity. Most such studies focus on several types of defect in PCs with unit cells consisting of two layers only,<sup>9–11</sup> and just a few deal with defects in general PCs.<sup>12</sup> Anyway, in all these studies the defect is vacancy, substitution, or interstitial.

In this paper we investigate another type of defect—twinning—in a general PC, in which the twins can be separated by any symmetrical structure. Unlike in most previous studies, we also take into account the magnetic properties of materials that have been demonstrated to be the principal influence on the properties of the

bandgap.<sup>13,14</sup> We explain for what is to our knowledge the first time the role of both refractive index and wave impedance of constituent materials on the properties of defect modes.

Our treatment is based on a transfer-matrix method. We consider general conditions, which include nonabsorbing isotropic materials with both dielectric and magnetic properties, oblique angle of incidence, and both transverse electric (TE) and transverse magnetic (TM) polarization. This method is described in Section 2 below. Section 3 is devoted to the derivation of analytical formulas for defect modes, for their tunability by thickness or by refractive index, and for enhancement of the field in the middle of the defect. The tuning capabilities with respect to rotation angle, thickness, refractive index, and impedance of the defect layer are discussed in Section 4. We restrict this discussion only to twins with elementary cells that consist of two homogeneous layers separated by another single homogeneous layer. Finally, in Section 5 we summarize the results.

## 2. TRANSFER-MATRIX METHOD FOR LAYERED DIELECTRIC STACKS

The transfer-matrix method has been widely used for the description of layered dielectric stacks and is described, e.g., in Ref. 15. However, as we deal with the less stud-

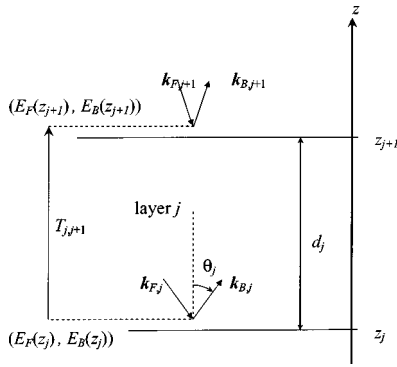


Fig. 1. Schematic of parameters of the transfer matrix method.

ied case of magnetic materials and with off-axis propagation, we briefly summarize our basic results here.

First, let us consider a stack of homogeneous nonabsorbing layers that have interfaces at positions  $z_j$  (see Fig. 1). Transfer matrix  $\mathbf{T}_{j,j+1}$  links the electric fields of waves propagating forward ( $E_F$ ) and backward ( $E_B$ ) at position  $z_j$  with those at position  $z_{j+1}$  (Fig. 1):

$$\begin{bmatrix} E_F(z_{j+1}) \\ E_B(z_{j+1}) \end{bmatrix} = \mathbf{T}_{j,j+1} \begin{bmatrix} E_F(z_j) \\ E_B(z_j) \end{bmatrix}. \quad (1)$$

This matrix can be written as

$$\mathbf{T}_{j,j+1} = \begin{bmatrix} T_{11} & T_{12} \\ T_{21} & T_{22} \end{bmatrix} = \frac{w_{j,j+1}}{2} \begin{bmatrix} (1 + x_{j,j+1}) \exp(-ik_{z,j}d_j) & (1 - x_{j,j+1}) \exp(+ik_{z,j}d_j) \\ (1 - x_{j,j+1}) \exp(-ik_{z,j}d_j) & (1 + x_{j,j+1}) \exp(+ik_{z,j}d_j) \end{bmatrix}, \quad (2)$$

where  $k_{z,j} = 2\pi f n_j \cos \theta_j / c$  is the  $z$  component of the wave vector in the  $j$ th layer;  $d_j$  and  $n_j = (\mu_j \epsilon_j)^{1/2}$  are, respectively, its thickness and refractive index,  $\theta_j$  is the angle between the wave vector and the  $z$  axis,  $f$  represents the frequency, and  $c$  is the speed of light in vacuum. The parameters  $w_{j,j+1}$  and  $x_{j,j+1}$  differ for TE and TM polarization:

$$\begin{aligned} \text{TE polarization:} \quad & w_{j,j+1} = 1, \\ & x_{j,j+1} = \frac{Z_{j+1} \cos \theta_j}{Z_j \cos \theta_{j+1}}, \\ \text{TM polarization:} \quad & w_{j,j+1} = \frac{\cos \theta_j}{\cos \theta_{j+1}}, \\ & x_{j,j+1} = \frac{Z_{j+1} \cos \theta_{j+1}}{Z_j \cos \theta_j}. \end{aligned} \quad (3)$$

$Z_j = (\mu_j / \epsilon_j)^{1/2}$  stands for the wave impedance of the  $j$ th layer. As we are dealing with nonabsorbing media, the elements of matrix  $\mathbf{T}_{j,j+1}$  satisfy the relations

$$T_{22} = T_{11}^*, \quad T_{12} = T_{21}^*. \quad (4)$$

These relations hold also for any stack of nonabsorbing layers. For such a structure, characterized by transfer matrix  $\mathbf{Q}$ , we can write

$$\begin{pmatrix} E_i \\ E_r \end{pmatrix} = \begin{bmatrix} Q_{11} & Q_{21}^* \\ Q_{21} & Q_{11}^* \end{bmatrix} \begin{pmatrix} E_t \\ 0 \end{pmatrix}, \quad (5)$$

where  $E_i$ ,  $E_r$ , and  $E_t$  stand for incident, reflected, and transmitted electric fields, respectively. It is then clear that the elements  $1/Q_{11}$  and  $Q_{21}/Q_{11}$  can be identified with complex transmission and reflection coefficients (in terms of electric field), respectively.

### 3. THEORETICAL DESCRIPTION OF ONE-DIMENSIONAL PHOTONIC CRYSTAL WITH A TWIN DEFECT

A schematic of the structure under investigation is shown in Fig. 2. Transfer matrix  $\mathbf{M}$  linking the fields in the middle of the defect structure and in the outer medium is given by

$$\mathbf{M} = \mathbf{A} \cdot \mathbf{S}^N \cdot \Delta, \quad (6)$$

where  $\mathbf{S}$  is the transfer matrix of a unit cell of the PC and  $\Delta$  is the transfer matrix of half of the defect structure (see Fig. 2). Matrix  $\mathbf{A}$  stands for the interface between the outer medium and an infinitesimally thin layer  $\tilde{L}$  (with same wave impedance and refractive index as the last layer  $L$  before the defect). This formal layer does not

change the physical properties of the structure, but it permits clear separation of the properties of the PC (as described by matrix  $\mathbf{S}^N$ ) from the coupling to the outer medium. The right-hand part of the structure is a mirror image of the left-hand part. Hence it is necessary to take opposite signs of all coordinates in Eq. (2), which is equivalent to taking the complex conjugate of Eq. (2). Transfer matrix  $\mathbf{P}$  of the whole structure is thus

$$\mathbf{P} = \mathbf{M} \cdot (\mathbf{M}^*)^{-1} = \mathbf{A} \cdot \mathbf{S}^N \cdot \Delta \cdot (\Delta^*)^{-1} \cdot (\mathbf{S}^*)^{-N} \cdot (\mathbf{A}^*)^{-1}. \quad (7)$$

It is appropriate to express transfer matrix  $\mathbf{S}^N$  in terms of complex transmission  $t \exp(i\tau)$  and reflection  $r \exp(i\rho)$  coefficients of the PC without a twinning defect:

$$\begin{pmatrix} E_i \\ E_r \end{pmatrix} = \mathbf{S}^N \begin{pmatrix} E_t \\ 0 \end{pmatrix}, \quad \mathbf{S}^N = \frac{1}{t} \begin{bmatrix} \exp(-i\tau) & r \exp[-i(\rho - \tau)] \\ r \exp[i(\rho - \tau)] & \exp(i\tau) \end{bmatrix}, \quad (8)$$

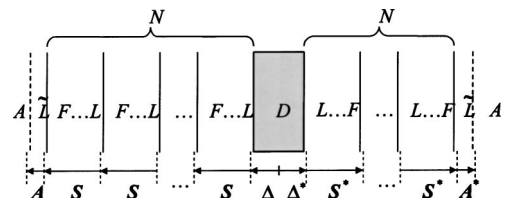


Fig. 2. Structure and corresponding transfer matrices:  $F...L$ , arbitrary sequence of layers starting with  $F$  and ending with  $L$ .

where  $r^2 + t^2 = 1$ , as we do not consider absorbing media. Indeed, we can clearly see that the first element of  $\mathbf{S}^N$  corresponds to the ratio  $E_i/E_r$  of the incident and transmitted electric fields, i.e., to the inverse of transmission coefficient  $t \exp(i\tau)$ . Other matrix elements are deduced in the same way. We now restrict ourselves only to frequencies for which the periodic structures on both sides of the defect exhibit a photonic bandgap. The presence of the structural defect can lead to an emergence of defect level(s) in the bandgap. The frequency of a defect mode corresponds to a vanishing reflectivity (high transmissivity) of the whole structure, i.e.,  $P_{21}/P_{11} = 0$ . In the limit of a perfect PC ( $r \rightarrow 1$ ), a direct but lengthy calculation shows that the numerator of  $P_{21}/P_{11}$  cancels out when

$$[\exp i(\rho - 2\tau)] = -\frac{\Delta_{21} \pm \Delta_{11}^*}{\Delta_{11} \pm \Delta_{21}^*}. \quad (9)$$

After simplification, it yields

$$2\tau - \rho \equiv 2 \arg(\Delta_{11} + \Delta_{21}^*) + \pi[2\pi], \quad (10a)$$

$$\equiv 2 \arg(\Delta_{11} - \Delta_{21}^*)[2\pi], \quad (10b)$$

where  $\arg(z)$  denotes the argument of complex number  $z$  and where  $[2\pi]$  indicates that the result is congruent with  $2\pi$ . Note that this expression does not depend on the properties of outer medium  $A$ . In the limit of a perfect PC, these defect modes coincide with the eigenmodes of

a transcendental equation for the frequency of defect modes. Nevertheless, the relative tunability of defect modes by the relative variation of the defect thickness yields

In fact, when the structure is irradiated at normal incidence, replacing  $d_D$  with  $n_D$  on the left-hand side of Eq. (12) leads to the relative tunability of defect modes by the relative variation of refractive index  $n_D$ .

Let us now focus on the enhancement of the electromagnetic field in the middle of the defect. For that purpose we consider the electric fields that are propagating forward ( $E_{\text{fwd}}$ ) and backward ( $E_{\text{bck}}$ ) in the middle of the defect. When the whole structure is irradiated only from the left side by a wave with electric field  $E_{\text{in}}$ , the sum and the difference of  $E_{\text{fwd}}$  and  $E_{\text{bck}}$ , which are respectively proportional to the magnitudes of the electric field ( $=E_{\text{fwd}} + E_{\text{bck}}$ ) and the magnetic induction [ $=(E_{\text{fwd}} - E_{\text{bck}})n_D/c$ ] in the middle of the defect, are given by

$$E_{\text{fwd}} \pm E_{\text{bck}} = \frac{1}{M_{11} \pm M_{21}^*} E_{\text{in}} \quad (13)$$

Let us examine this expression for frequencies that correspond to defect levels of a perfect PC [Eqs. (10)]. For even defect modes and upper signs in Eq. (13) or for odd defect modes and lower signs, the substitution for  $\mathbf{M}$  from Eq. (6) into Eq. (8) yields

$$\frac{E_{\text{fwd}} \pm E_{\text{bck}}}{E_{\text{in}}} = \frac{4}{w_{L,A} t \exp(-i\tau)(\Delta_{11} \pm \Delta_{21}^*)(1 + x_{L,A}) + \exp(i\tau)(\Delta_{21} \pm \Delta_{11}^*)(1 - x_{L,A})}. \quad (14)$$

the structure. When the condition of Eq. (10a) holds, matrix  $\mathbf{M}$  applied to vector  $(1, 1)$  leads to a null vector (which means that we deal with the standing modes of the structure). Hence Eq. (10a) describes even eigenmodes for the electric field (odd modes for the magnetic field). Analogously, odd eigenmodes are related to Eq. (10b): When this condition holds,  $\mathbf{M}$  applied to vector  $(1, -1)$  yields a null vector. The defect modes described by Eq. (10) thus coincide with the eigenmodes of the photonic structure.

If defect  $D$  is a homogeneous layer with thickness  $d_D$ , substitution of Eq. (2) for  $\Delta$  allows the results of Eqs. (10) to be simplified to the single expression

$$k_{z,D} d_D = m\pi + 2\varphi, \quad \varphi = \arctan(\tan \kappa/x_{D,L}),$$

$$\kappa = \frac{\rho(f) - 2\tau(f) + \pi}{2}, \quad (11)$$

where  $m$  is an integer. Even integers correspond to even defect modes, and odd integers correspond to odd modes. Owing to the frequency dependence of  $\rho$  and  $\tau$ , Eq. (11) is

When media  $A$  and  $L$  are the same (i.e.,  $w_{L,A} = 1$  and  $x_{L,A} = 1$ ), Eq. (14) is considerably simplified:

$$\frac{E_{\text{fwd}} \pm E_{\text{bck}}}{E_{\text{in}}} = \frac{2 \exp(i\tau)}{t \Delta_{11} \pm \Delta_{21}^*}. \quad (15)$$

For the opposite case (i.e., even parity and lower signs or odd parity and upper signs), Eq. (13) vanishes in the limit  $t \rightarrow 0$  (band gap of the PC), as it is directly proportional to  $t$ . For a homogeneous defect layer the enhancement factor in Eq. (15) reads as

$$\frac{1}{\Delta_{11} + \Delta_{21}^*} = \frac{1}{w_{D,L}} \left( \left\{ \begin{array}{c} 1 \\ x_{D,L} \end{array} \right\} \cos \frac{k_{z,D} d_D}{2} - i \left\{ \begin{array}{c} x_{D,L} \\ 1 \end{array} \right\} \sin \frac{k_{z,D} d_D}{2} \right)^{-1}. \quad (16)$$

Note that, for even modes, electric field  $E_{\text{fwd}} + E_{\text{bck}}$  is en-

$$\frac{d_D}{f} \frac{df}{dd_D} = \frac{1}{1 + \{(cx_{D,L}/\pi n_D d_D \cos \theta_D)[d(\rho - 2\tau)/df][1/((x_{D,L}^2 - 1)\cos(\rho - 2\tau) - (x_{D,L}^2 + 1))]\}}. \quad (12)$$

hanced, whereas it is the magnetic induction given by  $(E_{\text{fwd}} - E_{\text{bck}})n_D/c$  that is enhanced for odd modes.

#### 4. DISCUSSION

From a general point of view, Eqs. (10) offer the possibility of determining the frequencies of defect levels as soon as the parameters of the constituent PCs are known. For a single-layer defect [Eq. (11)] it is thus necessary to know the physical properties of both defect and surrounding medium (layer  $L$ ) and to determine either theoretically or experimentally<sup>16,17</sup> the dependence on frequency of phases  $\rho$  and  $\tau$ . Note that Eqs. (10) and (11) are general and were derived with only the assumption of perfect reflection of the structure surrounding the defect ( $r \rightarrow 1$ ). Hence a disordered PC can be described by these equations as well.

From now on, we focus on periodic structures and single-layer defects only, as depicted in Fig. 2. Indeed, this configuration coincides with that of a Fabry–Perot cavity (FPC) embedded in a complex material. Consequently the term  $\varphi$  that appears in Eq. (11) and that adds an additional phase shift to a simple FPC accounts for the distributed reflection of the electromagnetic wave on the PC. Phase shifts  $\rho$  and  $\tau$ , induced by the reflection and the transmission, respectively, of the PC, usually exhibit a linear behavior over a wide range of frequencies in the forbidden gap.<sup>16–18</sup> Hence an expansion of Eqs. (10) to the first order yields an explicit expression for the frequencies of defect modes:

$$f = \left[ m - \frac{2f_c}{\pi x_{D,L}} \kappa'(f_c) \right] \frac{c}{2n_D d_D - \frac{2c}{\pi x_{D,L}} \kappa'(f_c)}, \quad (17)$$

where  $\kappa' \equiv \partial \kappa / \partial f$  and where  $f_c$  is a root of the function  $\tan \kappa(f)$  inside the photonic bandgap:  $\kappa(f_c) \equiv 0[\pi]$ . We emphasize that this formula does not contain any frequency-dependent term. Consequently, as soon as the single parameter  $\kappa'(f_c)$  has been determined either theoretically or experimentally, it gives a good approximation of the frequency of the defect modes over a wide range of frequencies. The limited expansion into series leading to Eq. (17) is valid only for frequencies that satisfy  $|f - f_c| \ll \sqrt{3} \min(1, x_{D,L}) / |\kappa'(f_c)|$ ; hence the domain of validity of Eq. (17) becomes significantly narrower for small values of  $x_{D,L}$ .

We now discuss a PC that has elementary cells that consist of two layers of equal optical thickness. Here  $f_c = c/(2l_{\text{tot}})$  ( $l_{\text{tot}}$  is the optical thickness of a unit cell of the PC) is the central frequency of the bandgap. Moreover, such a structure provides the highest possible ratio of bandgap width to central frequency  $f_c$ .<sup>19</sup> Following the value of  $x_{D,L}$  [ $= Z_L/Z_D$  in the case of normal incidence; see Eq. (3)], defect-level positions show a qualitatively different behavior, as can be seen from Fig. 3(a). For  $x_{D,L} \gg 1$ , i.e., for impedance of the defect much lower than that of the last layer, phase shift  $\varphi$  becomes low and the defect modes thus approach those of the well-known FPC [dotted curves in Fig. 3(a)].

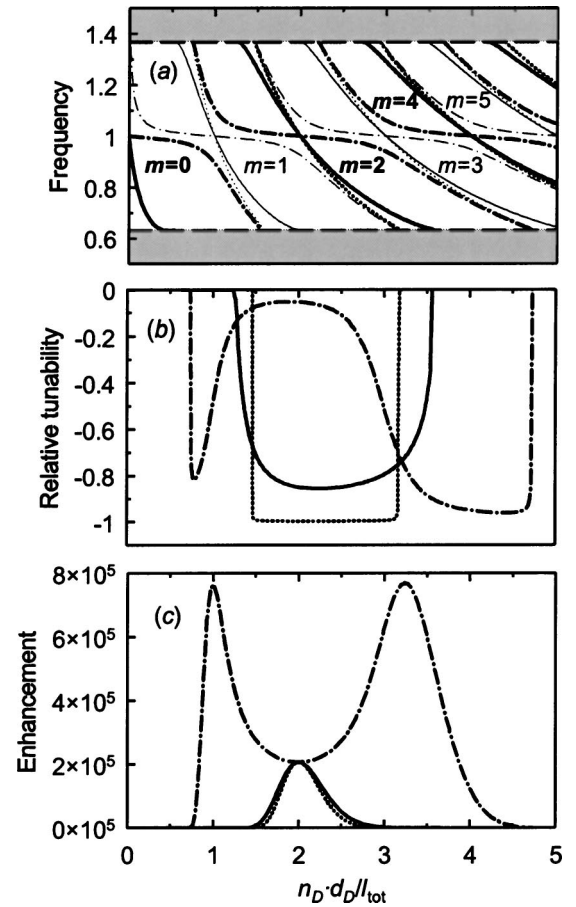


Fig. 3. (a) Dimensionless frequency [in units of  $c/(2l_{\text{tot}})$ ;  $l_{\text{tot}} = n_F d_F + n_L d_L$ ] of defect modes, (b) their relative tunability by optical thickness, and (c) enhancement of the electric field in the middle of the defect versus optical thickness of the defect. Dashed lines in (a) indicate band edges; thicker curves, even-parity modes; and thinner curves, odd-parity modes. The calculations were made with  $\theta = 0^\circ$  and  $Z_D = 0.0025$  (dotted curves),  $Z_D = 0.25$  (solid curves), and  $Z_D = 25$  (dashed-dotted curves). Parameters of the PC are  $n_F d_F = n_L d_L = l_{\text{tot}}/2$ ,  $Z_F = 1/3.4$ , and  $Z_L = Z_A = 1$ . The number of periods in (c) is  $N = 10$ . For clarity, only modes with  $m = 2$  are plotted in (b) and (c).

For the opposite ratio of impedances, the behavior is more complicated:  $\tan \kappa$  crosses zero for  $f = f_c$ ; i.e., the defect levels coincide with FPC modes without an additional phase shift for this frequency [Fig. 3(a)]. However, immediately as  $\tan \kappa$  becomes nonzero because of a small frequency variation, phase shift  $\varphi$  tends toward  $\pm \pi/2$  because the value of  $1/x_{D,L}$  is high [see Eq. (11)]. In other words, it is necessary to introduce a large change in optical thickness  $n_D d_D$  of the defect to tune the defect-level position in the vicinity of  $f_c$ . For frequencies farther apart from  $f_c$ , the  $m$ th mode [dashed-dotted curves in Fig. 3(a)] is attracted to the modes  $m - 1$  (for  $f > f_c$ ) and  $m + 1$  (for  $f < f_c$ ) of a FPC without an additional phase shift. There is thus a wide category of optical thicknesses of defects for which the tunability is practically excluded [Figs. 3(a) and 3(b)].

Indeed, as can easily be shown by Kramers–Kronig analysis,<sup>20</sup> the derivative of  $\rho - 2\tau$  versus frequency is always negative, and consequently the maximum relative tunability by relative variation of optical thickness [Eq.

(12)] is limited by  $-1$  [Fig. 3(b)]. Such a situation occurs in two cases:  $x_{D,L} \rightarrow 0$  ( $Z_D \rightarrow \infty$ ) and  $x_{D,L} \rightarrow \infty$  ( $Z_D \rightarrow 0$ ). However, the latter situation seems to be preferable, owing to the presence of fewer defect modes in the bandgap. This reduction in the number of defect modes with the decrease of  $Z_D$  clearly appears in Figs. 3(a) and 4(a).

Enhancement of the electric field inside the defect is of great interest in conjunction with nonlinear phenomena in PCs.<sup>21,22</sup> Because of the presence of the factor  $1/t$  in Eq. (15), the electric field enhancement is proportional to the quality of the PC (e.g., it grows rapidly with the number of periods), whereas the factor  $1/(\Delta_{11} \pm \Delta_{21}^*)$  stands for the enhancement that is due to the properties of the defect. For a single-layer defect [Eq. (16)] the magnitude of the latter enhancement factor may vary from  $1/w_{D,L}$  to  $1/(w_{D,L}x_{D,L})$ . The last term then causes an increase in the maximum enhancement when the impedance of the defect is larger than that of the last layer  $L$  [Fig. 3(c)]. In contrast, for  $n_D d_D = m l_{\text{tot}}$  the enhancement factor does not depend any more on impedance  $Z_D$  at normal incidence.

Let us now consider the tunability of defect modes directly by impedance. This is a fundamental mechanism of tunability in microwave devices for which it is considerably easier to vary the impedance than the refractive index of a defect. As shown in Fig. 4, such tunability is an order of magnitude lower than that by optical thickness. Depending on the position in the bandgap with respect to  $f_c$ , the frequency of the defect modes either increases with impedance ( $f < f_c$ ) or decreases ( $f > f_c$ ). Indeed, the right-hand side of Eq. (11) is a monotonic function of  $x_{D,L}$ , increasing or decreasing according to the sign of  $\tan \kappa$  and intersecting zero for  $f = f_c$ . In the limit

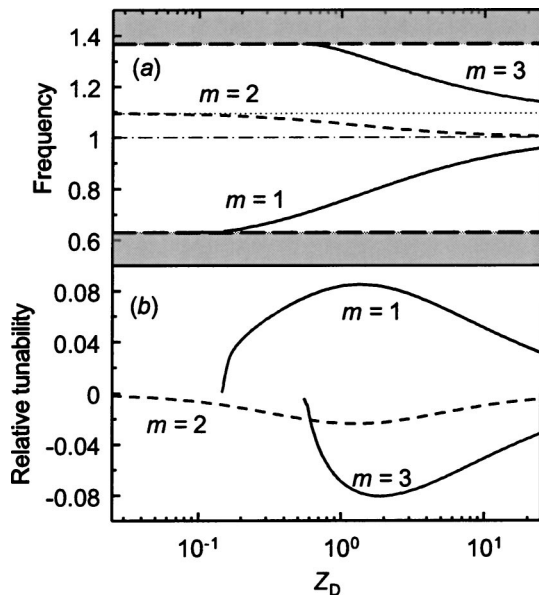


Fig. 4. (a) Dimensionless frequency of defect modes and (b) their relative tunability by impedance versus impedance of the defect. Long-dashed lines indicate band edges; Dashed-dotted curve, middle of the gap; dotted curve, asymptotic limits of defect levels when  $Z_D \rightarrow 0$  ( $m = 2$ ) or  $Z_D \rightarrow \infty$  ( $m = 3$ ). The calculations were performed with  $n_D d_D = 1.824 l_{\text{tot}}$  and  $\theta = 0^\circ$ ; other parameters are the same as in Fig. 3.

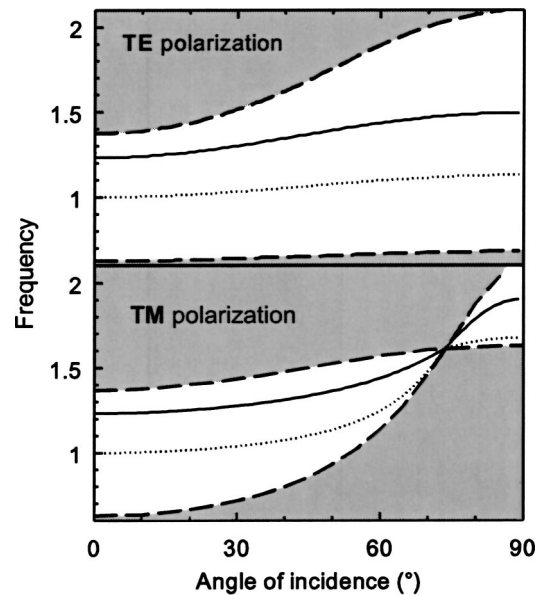


Fig. 5. Dimensionless frequency of a defect mode as a function of angle of incidence  $\theta$  on the PC. Dashed curves, band edges; dotted and solid curves,  $n_D d_D = 0.735 l_{\text{tot}}$  and  $n_D d_D = l_{\text{tot}}$ , respectively. For both polarizations  $Z_D = 0.25$  and  $n_A = 1$ . Other parameters are the same as in Fig. 3.

of high impedance, the frequency of the  $m$ th defect mode reaches asymptotically either  $f_c$  or mode  $m - 1$  (for  $f > f_c$ ) or  $m + 1$  (for  $f < f_c$ ) of a FPC without an additional phase shift. Both limits can be clearly seen in Fig. 3(a) when the optical thickness is kept while the impedance is varied. As shown in Fig. 4(a), new defect modes arise in the bandgap with increasing impedance.

From a practical point of view, tunability of the defect level could be simply achieved by rotation of the PC (Fig. 5). However, the tunability is low for both polarizations at small angles of incidence. TM polarization offers slightly better tunability at higher angles, but simultaneously with increasing angle the bandgap gets narrower.

## 5. SUMMARY

We have derived general analytical expressions for the frequencies of defect modes for twinning in an arbitrary structure that exhibits a forbidden gap. We focused on the case of a PC with a two-layer elementary cell surrounding a single homogeneous defect layer, and we explained the influence of impedance on the position and tunability of defect modes as well as on the enhancement of the electromagnetic field in the middle of the defect layer. Tunability by variation of optical thickness, impedance, and angle of incidence was also discussed.

## ACKNOWLEDGMENTS

This study was supported by the French Ministry of Education through an Action Concertée Incitative.

L. Duvillaret's e-mail address is [duvillaret@univ-savoie.fr](mailto:duvillaret@univ-savoie.fr).

## REFERENCES

1. E. Yablonovitch, "Inhibited spontaneous emission in solid-state physics and electronics," *Phys. Rev. Lett.* **58**, 2059–2062 (1987).
2. A. Chelnokov, S. Rowson, J. M. Lourtioz, L. Duvillaret, and J. L. Coutaz, "Terahertz characterisation of mechanically machined 3D photonic crystal," *Electron. Lett.* **33**, 1981–1983 (1997).
3. H. Míguez, C. López, F. Meseguer, A. Blanco, L. Vázquez, R. Mayoral, M. Ocaña, V. Fornés, and A. Mifsud, "Photonic crystal properties of packed submicrometric SiO<sub>2</sub> spheres," *Appl. Phys. Lett.* **71**, 1148–1150 (1997).
4. A. de Lustrac, F. Gadot, S. Cabaret, J.-M. Lourtioz, T. Brillat, A. Priou, and E. Akmansoy, "Experimental demonstration of electrically controllable photonic crystals at centimeter wavelengths," *Appl. Phys. Lett.* **75**, 1625–1627 (1999).
5. A. Chelnokov, S. Rowson, J. M. Lourtioz, L. Duvillaret, and J. L. Coutaz, "Light controllable defect modes in three-dimensional photonic crystal," *Electron. Lett.* **34**, 1965–1967 (1998).
6. H.-Y. Lee and T. Yao, "Design and evaluation of omnidirectional one-dimensional photonic crystals," *J. Appl. Phys.* **93**, 819–830 (2003).
7. M. Okano, A. Chutinan, and S. Noda, "Analysis and design of single-defect cavities in a three-dimensional photonic crystal," *Phys. Rev. B* **66**, 165211 (2002).
8. K. Sakoda and H. Shiroma, "Numerical method for localized defect modes in photonic lattices," *Phys. Rev. B* **56**, 4830–4835 (1997).
9. D. R. Smith, R. Dalichaouch, N. Kroll, S. Schultz, S. L. McCall, and P. M. Platzman, "Photonic band structure and defects in one and two dimensions," *J. Opt. Soc. Am. B* **10**, 314–321 (1993).
10. H. Miyazaki, Y. Jimba, C. Y. Kim, and T. Watanabe, "Defects and photonic wells in one-dimensional photonic lattices," *J. Phys. Soc. Jpn.* **65**, 3842–3852 (1996).
11. Y. C. Tsai, K. W. K. Shung, and S. C. Gou, "Impurity modes in one-dimensional photonic crystals—analytic approach," *J. Mod. Opt.* **45**, 2147–2157 (1998).
12. A. Figotin and V. Gortentsveig, "Localized electromagnetic waves in a layered periodic dielectric medium with a defect," *Phys. Rev. B* **58**, 180–188 (1998).
13. M. M. Sigalas, C. M. Soukoulis, R. Biwas, and K. M. Ho, "Effect of the magnetic permeability on photonic band gaps," *Phys. Rev. B* **56**, 959–962 (1997).
14. C.-S. Kee, J.-E. Kim, H. Y. Park, S. J. Kim, H. C. Song, Y. S. Kwon, N. H. Myung, S. Y. Shin, and H. Lim, "Essential parameter in the formation of photonic band gaps," *Phys. Rev. E* **59**, 4695–4698 (1999).
15. M. Born and E. Wolf, *Principles of Optics*, 7th ed. (Cambridge U. Press, Cambridge, 1999), Sect. 1.6, pp. 54–74.
16. E. Ozbay and B. Temelkuran, "Reflection properties and defect formation in photonic crystals," *Appl. Phys. Lett.* **69**, 743–745 (1996).
17. T. Aoki, M. W. Takeda, J. W. Haus, Z. Yuan, M. Tani, K. Sakai, N. Kawai, and K. Inoue, "Terahertz time-domain study of a pseudo-simple-cubic photonic lattice," *Phys. Rev. B* **64**, 045106 (2001).
18. N. Tsurumachi, S. Yamashita, N. Muroi, T. Fuji, T. Hattori, and H. Nakatsuka, "Enhancement of nonlinear optical effect in one-dimensional photonic crystal structures," *Jpn. J. Appl. Phys., Part 1* **38**, 6302–6308 (1999).
19. J. N. Winn, Y. Fink, S. Fan, and J. D. Joannopoulos, "Omnidirectional reflection from a one-dimensional photonic crystal," *Opt. Lett.* **23**, 1573–1575 (1998).
20. H. Němec, P. Kužel, F. Garet, and L. Duvillaret, "Time-domain terahertz study of defect formation in one-dimensional photonic crystals," *Appl. Opt.* (to be published).
21. T. Hattori, N. Tsurumachi, and H. Nakatsuka, "Analysis of optical nonlinearity by defect states in one-dimensional photonic crystals," *J. Opt. Soc. Am. B* **14**, 348–355 (1997).
22. B. Shi, Z. M. Jiang, X. F. Zhou, and X. Wang, "A two-dimensional nonlinear photonic crystal for strong second harmonic generation," *J. Appl. Phys.* **91**, 6769–6771 (2002).